JACS
JOURNAL OF THE AMERICAN CHEMICAL SOCIETY
Communication
pubs.acs.org/JACS

A Mononuclear Non-Heme Manganese(IV)−Oxo Complex Binding Redox-Inactive Metal Ions

Junying Chen,[†] Yong-Min Lee,[†] Katherine M. Davis,[‡] Xiujuan Wu,[†] Mi Sook Seo,[†] Kyung-Bin Cho,[†] Heejung Yoon,[†] Young Jun Park,[†] Shunichi Fukuzumi,*[,†,§] Yulia N. Pushkar,*[,‡] and Wonwoo Nam*[,†]

[†]Department of Bioinspired Science, Chemistry and Nano Science, Ewha Womans University, Seoul 120-750, Korea

[‡]Department of Physics, Purdue University, 525 Northwestern Avenue, West Lafayette, Indiana 47907, United States

[§]Department of Material and Life Science, Graduate School of Engineering, Osaka University, and ALCA, Japan Science and Technology Agency (JST), Suita, Osaka 565-0871, Japan

Supporting Information

ABSTRACT: Redox-inactive metal ions play pivotal roles in regulating the reactivities of high-valent metal−oxo species in a variety of enzymatic and chemical reactions. A mononuclear non-heme Mn(IV)−oxo complex bearing a pentadentate N_5 ligand has been synthesized and used in the synthesis of a Mn(IV)−oxo complex binding scandium ions. The Mn(IV)−oxo complexes were characterized with various spectroscopic methods. The reactivities of the Mn(IV)−oxo complex are markedly influenced by binding of Sc^{3+} ions in oxidation reactions, such as a ∼2200-fold increase in the rate of oxidation of thioanisole (i.e., oxygen atom transfer) but a ∼180-fold decrease in the rate of C−H bond activation of 1,4-cyclohexadiene (i.e., hydrogen atom transfer). The present results provide the first example of a non-heme Mn(IV)−oxo complex binding redox-inactive metal ions that shows a contrasting effect of the redox-inactive metal ions on the reactivities of metal−oxo species in the oxygen atom transfer and hydrogen atom transfer reactions.

High-valent metal−oxo species have been invoked as key intermediates in the dioxygen O−O bond-cleavage and bond-formation reactions by a number of metalloenzymes, such as heme and non-heme iron oxygenases for the oxidation of organic substrates and Photosystem II (PS II) for the oxidation of water.[1−3] In biomimetic studies, a number of iron−oxo and manganese−oxo complexes bearing porphyrin, corrole, corrolazine, and non-porphyrin ligands have been synthesized and characterized with various spectroscopic techniques and X-ray crystallography.[4] Their reactivities have also been investigated in a variety of oxygen atom transfer (OAT), hydrogen atom transfer (HAT), and electron transfer (ET) reactions.[4]

Metal ions that function as Lewis acids play pivotal roles in tuning the reactivities of metal−oxo complexes in a variety of chemical transformations, such as OAT and ET reactions.[5] It is widely accepted that in PS II, a redox-inactive Ca^{2+} ion acts as an essential cofactor for the oxidation of water to evolve dioxygen at the manganese−calcium (Mn_4CaO_5) active site.[6] Although the exact functional role of the Ca^{2+} ion remains elusive, it has been proposed that the presence of a redox-inactive Ca^{2+} ion facilitates the O−O bond-formation step by a presumed Mn(V)−oxo species.[7]

We recently reported the first crystal structure of a non-heme Fe(IV)−oxo complex binding a Sc^{3+} ion.[8] We also showed that the rates of OAT and ET reactions of non-heme Fe(IV)−oxo complexes are markedly increased upon addition of redox-inactive metal ions.[9] More recently, Goldberg and co-workers reported the influence of a redox-inactive Zn^{2+} ion on a valence tautomerization of a Mn(V)−oxo corrolazine complex and its enhanced ET and HAT reactivity.[10] As part of our ongoing efforts to understand the effects of redox-inactive metal ions on the reactivities of metal−oxo species, we synthesized, characterized, and investigated the reactivities of a non-heme Mn(IV)−oxo complex and its Sc^{3+} ion-binding species (Figure 1). Here we report the first spectroscopic evidence for the binding of Sc^{3+} ions by a mononuclear non-heme Mn(IV)−oxo complex and the contrasting effect of metal ions on the OAT and HAT reactions of the Sc^{3+} ion-binding Mn(IV)−oxo complex.

The starting manganese complex, $[Mn^{II}(N4Py)(CF_3SO_3)]^+$ (**1**) [N4Py = *N*,*N*-bis(2-pyridylmethyl)-*N*-bis(2-pyridyl)-methylamine; Figure 1d], was synthesized and characterized with electrospray ionization mass spectrometry (ESI-MS), electron paramagnetic resonance (EPR) spectroscopy, and X-ray crystallography [see the Experimental Section, Figures S1 and S2, and Tables S1 and S2 in the Supporting Information (SI)]. Addition of 4 equiv iodosylbenzene (PhIO) to a solution of **1** (1 mM) in CF_3CH_2OH at 25 °C afforded a greenish-yellow complex, **2**, with an absorption band at 940 nm ($\varepsilon \approx 250$ M^{-1} cm^{-1}) (Figure 2). The metastable intermediate ($t_{1/2} \approx 2$ h at 25 °C) was characterized with various spectroscopic techniques. The X-band EPR spectrum of **2** shows signals that are characteristic of $S = {}^3/_2$ Mn^{IV} (Figure S3),[11] and the $S = {}^3/_2$ spin state of **2** was confirmed using the modified NMR method of Evans (Experimental Section).[12] The ESI-MS spectrum of **2** exhibits a prominent ion peak at *m*/*z* 587.0 (Figure S4) whose mass and isotope distribution patterns correspond to $[Mn^{IV}(O)(N4Py)(CF_3SO_3)]^+$ (calcd *m*/*z* 587.1). Upon introduction of ^{18}O into **2** using $PhI^{18}O$, a

Received: December 12, 2012
Published: January 16, 2013

   dx.doi.org/10.1021/ja312113p | *J. Am. Chem. Soc.* 2013, 135, 6388−6391

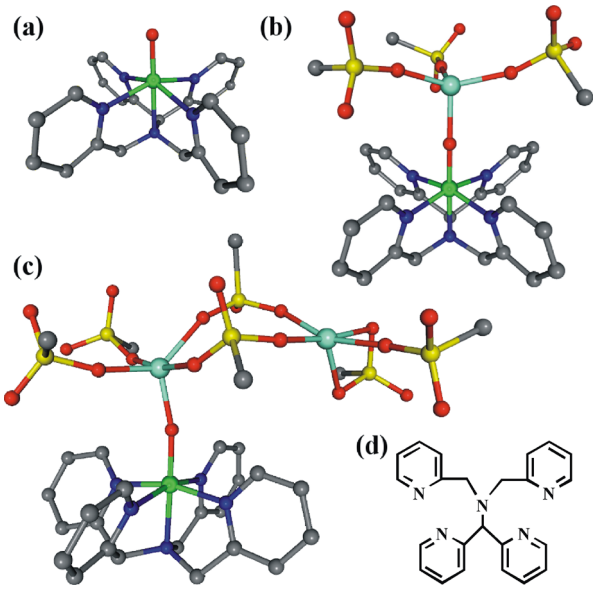

Figure 1. (a–c) DFT-optimized structures of (a) $[Mn^{IV}(O)(N4Py)]^{2+}$ (**2**), (b) $[Mn^{IV}(O)(N4Py)–Sc(CF_3SO_3)_3]^{2+}$ (**3**), and (c) $[Mn^{IV}(O)(N4Py)–Sc(CF_3SO_3)_3–Sc(CF_3SO_3)_3]^{2+}$ (**4**), calculated at the B3LYP/LACVP level in the solvent phase. The Mn–O bond lengths of **2**, **3**, and **4** were calculated to be 1.67, 1.74, and 1.74 Å, respectively (see the DFT Calculations Section in the SI for computational details). H atoms in N4Py and F atoms in the $CF_3SO_3^-$ counterions have been omitted for clarity (Mn, green; N, blue; O, red; C, black; Sc, aquamarine; S, yellow). (d) Structure of the N4Py ligand.

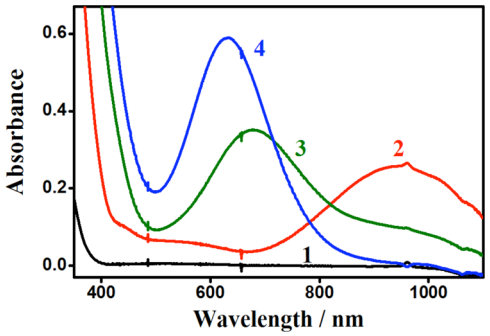

Figure 2. UV–vis spectra of $[Mn^{II}(N4Py)(CF_3SO_3)]^+$ (**1**) (black line; 1.0 mM), $[Mn^{IV}(O)(N4Py)]^{2+}$ (**2**) (red line; addition of 4 equiv PhIO to **1**), $[Mn^{IV}(O)(N4Py)]^{2+}–Sc^{3+}$ (**3**) (green line; addition of 1 equiv of Sc^{3+} to **2**), and $[Mn^{IV}(O)(N4Py)]^{2+}–2Sc^{3+}$ (**4**) (blue line; addition of 5 equiv of Sc^{3+} to **3**) in CF_3CH_2OH at 25 °C.

mass shift from m/z 587.0 to 589.0 was observed (Figure S4), indicating that **2** contains an oxygen atom.

Comparison of the X-ray absorption near-edge structure (XANES) at the Mn K-edges for **1** and **2** demonstrates a large shift to higher energy for **2**, confirming its Mn^{IV} oxidation state (Figure 3a).[11] Extended X-ray absorption fine structure (EXAFS) shows that the first peak corresponding to Mn–O,N interactions in the first coordination sphere is shifted to a shorter apparent distance in **2** relative to **1**. This change can be rationalized as shortening of the Mn–O,N bond distances in **2**, and fits to the EXAFS data indicate the presence of a 1.70 Å Mn=O interaction as well as shortening of the Mn–N distance [Table S3; also see the 1.67 Å Mn–O distance from density functional theory (DFT) calculations in Figure 1a].[11,13] On the basis of the spectroscopic characterization presented

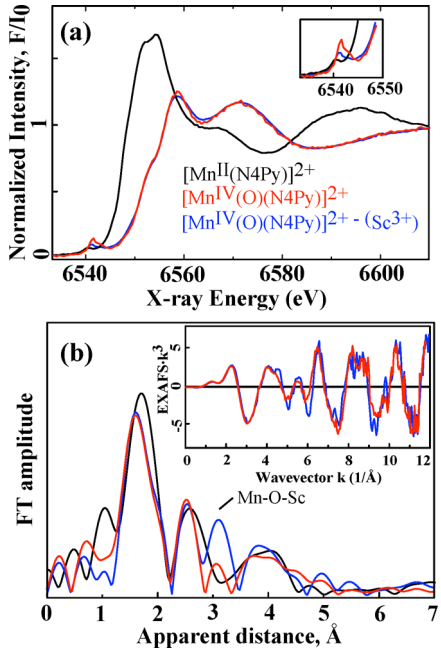

Figure 3. (a) Normalized Mn K-edge XANES of **1** (black), **2** (red), and **4** (blue). The inset shows magnified pre-edge features. (b) Overlay of the Fourier transforms (k = 3.5–11.3 $Å^{-1}$) of the EXAFS data for **1** (black), **2** (red), and **4** (blue). The inset shows k-space data for **2** and **4**. (Fits are shown in Table S3 and Figure S8.)

above, **2** is assigned as the mononuclear Mn(IV)–oxo complex $[Mn^{IV}(O)(N4Py)]^{2+}$ (Figure 1a).

Addition of Sc^{3+} ions to the solution of **2** resulted in a stepwise change in the absorption spectrum (Figure 2 and Figure S5a). The absorption band at 940 nm due to **2** changed to a new absorption band at 680 nm with a well-defined isosbestic point at 817 nm upon the addition of up to 1 equiv of Sc^{3+} (Figure 2 and Figure S5b). Further addition of Sc^{3+} ions (up to ~5 equiv of Sc^{3+}) to the resulting solution moved the absorption band from 680 to 635 nm (Figure 2 and Figure S5b). Such spectral changes of **2** upon addition of Sc^{3+} ions suggest that a Mn(IV)–oxo complex with one bound Sc^{3+} ion (**3**) is produced initially (eq 1) and then is converted to a Mn(IV)–oxo complex with two bound Sc^{3+} ions (**4**) (eq 2). The equilibrium constant K_2 for binding of the second Sc^{3+} ion to give **4** was determined from the titration experiment to be 6.1×10^3 M^{-1} (Figure S5b); K_1 for binding of the first Sc^{3+} ion to give **3** was too large to be determined accurately ($K_1 \gg 10^4$ M^{-1}).

$$\underset{(\mathbf{2})}{[Mn^{IV}(O)(N4Py)]^{2+}} + Sc^{3+} \overset{K_1}{\rightleftarrows} \underset{(\mathbf{3})}{[Mn^{IV}(O)(N4Py)]^{2+}–Sc^{3+}} \quad (1)$$

$$\underset{(\mathbf{3})}{[Mn^{IV}(O)(N4Py)]^{2+}–Sc^{3+}} + Sc^{3+} \overset{K_2}{\rightleftarrows} \underset{(\mathbf{4})}{[Mn^{IV}(O)(N4Py)]^{2+}–2Sc^{3+}} \quad (2)$$

The highly stable intermediates **3** ($t_{1/2}$ ≈ 12 h at 25 °C) and **4** ($t_{1/2}$ ≈ 1 day at 25 °C) were characterized with various spectroscopic techniques. The EPR spectra of **3** and **4** (Figure S3), along with the Evans NMR method (see the Experimental

dx.doi.org/10.1021/ja312113p | J. Am. Chem. Soc. 2013, 135, 6388–6391

Section),[12] indicate the Mn^{IV} spin state to be $S = {}^3/_2$.[11] The ESI-MS spectrum of **3** exhibits ion peaks at m/z 1028.9 and 1078.9 that shift to 1030.9 and 1080.9 upon use of $PhI^{18}O$ (Figure S6), suggesting that **3** contains one oxygen atom and binds one Sc^{3+} ion (Figure 1b). The ESI-MS spectrum of **4** exhibits ion peaks at m/z 1028.9, 1078.9, 1520.6, and 1570.5 (Figure S7); the latter two peaks correspond to $[Mn^{IV}(O)(N4Py)]^{2+}$ with two Sc^{3+} ions. Upon introduction of ^{18}O into **4** using $PhI^{18}O$, a shift of m/z 2 in the ion peaks was observed (Figure S7b), indicating that **4** contains one oxygen atom (Figure 1c).

4 was further characterized with XANES/EXAFS. The binding of Sc^{3+} to form **4** does not change the position of the Mn K-edge (Figure 3a), confirming an unchanged Mn^{IV} oxidation state, as shown in the EPR results (Figure S3). However, the pre-edge intensity is slightly lower in **4** relative to **2** (see the Figure 3a inset), indicating differences in the electronic structure due to Sc^{3+} binding. Because 1s → 3d transitions are dipole-forbidden, the pre-edge intensity arises mostly from quadrupole transitions and transitions to orbitals with mixed Mn 3d and ligand 2p character. The decreased pre-edge intensity in **4** suggests that Sc^{3+} binding decreases the mixing of Mn 3d and O 2p orbitals. EXAFS analysis did not show elongation of the Mn−O distance in **4** (Table S3), likely because the small distance change is within the resolution of our measurements. The EXAFS data in Figure 3b show the presence of an additional peak for **4**. This peak was assigned to a Mn−Sc distance of 3.5 Å, as was confirmed by the fits in Table S3. The EXAFS fit quality was better for the model with one Mn−Sc interaction (Figure S8). DFT calculations support similar geometries around the Mn center in **3** and **4** (Table S6), suggesting one direct Mn−Sc interaction. As shown in the DFT-optimized structures (Figure 1b,c), there is one direct bond between a Sc^{3+} ion and the Mn−O moiety in **3** and **4**.[14] In addition, the Mn−Sc distances in **3** and **4** were calculated to be 3.65 and 3.66 Å, respectively, which are in good agreement with the EXAFS results (vide supra). On the basis of the spectroscopic characterization discussed above, **3** is proposed to have one Sc^{3+} ion directly bound to the $[Mn^{IV}(O)(N4Py)]^{2+}$ complex (Figure 1b); likewise, **4**, which contains two Sc^{3+} ions, has one Sc^{3+} ion bound directly to the Mn−oxo moiety, with the other Sc^{3+} ion located in the secondary coordination sphere (Figure 1c).[14]

We then compared the reactivities of **2**, **3**, and **4** in OAT and HAT reactions. The reactivities of the Mn(IV)−oxo complexes were first investigated kinetically in OAT, such as the oxidation of thioanisole. Upon addition of thioanisole to solutions of **2**, **3**, and **4**, the intermediates reverted back to the starting Mn(II) complex, with **4** being much more reactive than **2** [Figure 4; see Figures S9 and S10 for EPR and ESI-MS spectra, respectively,

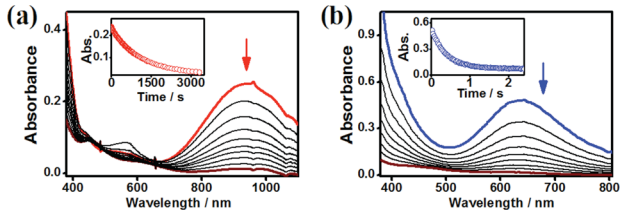

Figure 4. UV−vis spectral changes for (a) **2** (1.0 mM) and (b) **4** (1.0 mM) upon addition of thioanisole (0.10 M) at 0 °C. The insets show the time traces monitored at (a) 940 nm for **2** and (b) 635 nm for **4**.

for the Mn(II) product formation].[15] The conversion of Mn(IV)−oxo to Mn(II) species indicates that the oxidation of sulfide by the Mn(IV)−oxo complexes occurs via a two-electron oxidation process.[11] Product analysis of the reaction solutions revealed the formation of methyl phenyl sulfoxide in quantitative yield. The second-order rate constants determined in the reactions of **2** and **4** were 9.2×10^{-3} and 2.0×10^{1} M^{-1} s^{-1}, respectively, at 0 °C (Figure S11),[15] demonstrating that the reactivity of the Mn(IV)−oxo complex in the OAT reaction is markedly enhanced by binding of Sc^{3+} ions (i.e., ∼2200-fold increase in reactivity). The high reactivity of the Mn(IV)−oxo species with bound Sc^{3+} ions was also observed in the reactions of para-substituted thioanisoles, and ρ values of −4.6 and −5.6 were obtained for the reactions of **2** and **4**, respectively (Table S4 and Figure S12). In addition, plots of log k versus the one-electron oxidation potentials of thioanisoles afforded a good linear correlation (Table S4 and Figure S13).

The reactivities of **2**, **3**, and **4** were also investigated kinetically in HAT, such as the C−H bond activation of 1,4-cyclohexadiene (CHD). Addition of CHD to solutions of **2**, **3**, and **4** afforded a Mn(III) species with the reactivity order **2** > **3** > **4** and with isosbestic points at 400 and 715 nm for **2**, 433 and 575 nm for **3**, and 450 and 525 nm for **4** [Figure 5; see Figures

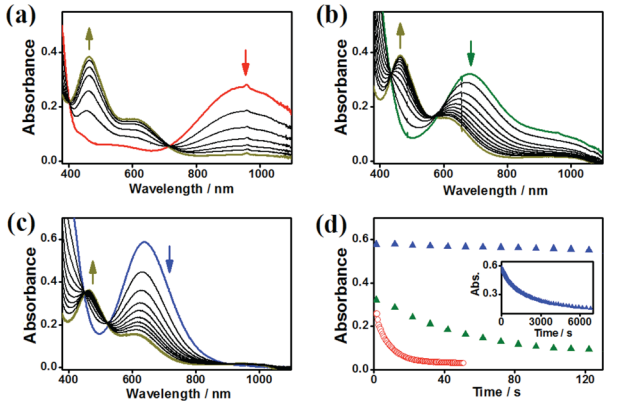

Figure 5. (a−c) UV−vis spectral changes for (a) **2**, (b) **3**, and (c) **4** (each 1.0 mM) upon addition of CHD (20 mM) at 25 °C. (d) Time traces monitored at 940 nm for **2** (red ○), 680 nm for **3** (green ▲), and 635 nm for **4** (blue ▲). The inset shows the time trace for **4** for longer times.

S9 and S10 for EPR and ESI-MS spectra, respectively, for the Mn(III) product formation]; we recently reported experimental and theoretical results for the formation of Mn(III) products in the C−H bond activation of alkanes by non-heme Mn(IV)−oxo complexes.[11,13] Product analysis of the reaction solutions of **2**−**4** revealed the formation of benzene as the sole product, as observed in the oxidation of CHD by other metal−oxo complexes.[16] The second-order rate constants determined in the reactions of **2**−**4** were 6.2, 1.2, and 3.5×10^{-2} M^{-1} s^{-1}, respectively, at 25 °C (Figure S14), indicating that the reactivity of the Mn(IV)−oxo complex was diminished by factors of ∼5 and ∼180 upon binding of one and two Sc^{3+} ions, respectively. These results are in sharp contrast to those for the OAT reaction, in which the binding of Sc^{3+} ions markedly increased the reactivity of the Mn(IV)−oxo species (vide supra). In addition, such a significant deceleration in the rate of C−H bond activation by the Sc^{3+}-binding Mn(IV)−oxo complex ions is different from the results reported for HAT reactions

dx.doi.org/10.1021/ja312113p | J. Am. Chem. Soc. 2013, 135, 6388−6391

involving a Zn^{2+}-binding Mn(IV)−oxo complex[10] and a Sc^{3+}-binding $[Fe^{IV}(O)(N4Py)]^{2+}$ complex.[17]

The contrasting effects of Sc^{3+} ion binding observed in the OAT and HAT reactions by Mn(IV)−oxo species might be explained by the difference in their reaction mechanisms. In the case of OAT, ET from the thioanisole to **4**, which may be the rate-determining step, is followed by a fast OAT step, as shown in Sc^{3+}-promoted OAT reactions by $[Fe^{IV}(O)(N4Py)]^{2+}$.[9] The proposed ET pathway is supported by the good linear correlation between the reaction rate constants and the E_{ox} values for the para-substituted thioanisoles (Figure S13).[9b,18] Such an ET pathway requires only a little interaction between **4** and the thioanisole, which is rather insensitive to the steric effect caused by the Sc^{3+} ions bound to the Mn−oxo moiety. In contrast, the HAT reaction requires significant interaction in the substrate C−H bond activation by the Mn−oxo moiety in **3** or **4**, which would be hindered by the Sc^{3+} ions bound to the Mn−oxo moiety (see Figure 1).

In summary, we have reported the synthesis, characterization, and reactivity of mononuclear non-heme Mn(IV)−oxo complexes binding Sc^{3+} ions and the contrasting effect of the bound metal ion on the reactivities of the Mn(IV)−oxo species in OAT and HAT reactions. The increased reactivity in OAT is rationalized by the involvement of an ET pathway, whereas the decreased reactivity in HAT is interpreted in terms of the steric hindrance caused by the Sc^{3+} ions bound to the Mn−oxo moiety. The present results provide an example demonstrating a diverse effects of a redox-inactive metal ion on the reactivities of high-valent metal−oxo species in oxidation reactions.

■ ASSOCIATED CONTENT

Supporting Information

Experimental section, crystal structure of **1**-CF_3SO_3 (CIF), spectroscopic data for **1**−**4**, reactivity data for **2**−**4**, and DFT Calculations section. This material is available free of charge via the Internet at http://pubs.acs.org.

■ AUTHOR INFORMATION

Corresponding Author

fukuzumi@chem.eng.osaka-u.ac.jp; ypushkar@purdue.edu; wwnam@ewha.ac.kr

Notes

The authors declare no competing financial interest.

■ ACKNOWLEDGMENTS

The authors gratefully acknowledge research support of this work by the NRF of Korea through CRI, WCU (R31-2008-000-10010-0), GRL (2010-00353), Basic Research Program (2010-0002558) (to M.S.S.) and by a Grant-in-Aid (20108010) and a Global COE Program from MEXT, Japan (to S.F.). The research at Purdue was supported by DOE-BES (DE-FG02-10ER16184 to Y.N.P.) and an NSF Graduate Research Fellowship (0833366 to K.M.D.). Synchrotron facilities were provided by the APS at Argonne National Laboratory, operated by DOE-BES under Contract DE-AC02-06CH11357. We thank Dr. Steve Heald and Dr. Dale Brewer for help with experiments at BM-20, APS.

■ REFERENCES

(1) Nam, W. *Acc. Chem. Res.* **2007**, *40*, 465 and references therein.

(2) Hammarström, L.; Hammes-Schiffer, S. *Acc. Chem. Res.* **2009**, *42*, 1859 and references therein.

(3) (a) Rittle, J.; Green, M. T. *Science* **2010**, *330*, 933. (b) Abu-Omar, M. M.; Loaiza, A.; Hontzeas, N. *Chem. Rev.* **2005**, *105*, 2227. (c) Krebs, C.; Fujimori, D. G.; Walsh, C. T.; Bollinger, J. M., Jr. *Acc. Chem. Res.* **2007**, *40*, 484. (d) Bruijnincx, P. C. A.; van Koten, G.; Klein Gebbink, R. J. M. *Chem. Soc. Rev.* **2008**, *37*, 2716.

(4) (a) Nam, W. *Acc. Chem. Res.* **2007**, *40*, 522. (b) Goldberg, D. P. *Acc. Chem. Res.* **2007**, *40*, 626. (c) Aviv, I.; Gross, Z. *Chem. Commun.* **2007**, 1987. (d) Gunay, A.; Theopold, K. H. *Chem. Rev.* **2010**, *110*, 1060. (e) Borovik, A. S. *Chem. Soc. Rev.* **2011**, *40*, 1870. (f) Mayer, J. M. *Acc. Chem. Res.* **2011**, *44*, 36. (g) de Visser, S. P.; Rohde, J.-U.; Lee, Y.-M.; Cho, J.; Nam, W. *Coord. Chem. Rev.* **2013**, *257*, 381.

(5) (a) Pfaff, F. F.; Kundu, S.; Risch, M.; Pandian, S.; Heims, F.; Pryjomska-Ray, I.; Haack, P.; Metzinger, R.; Bill, E.; Dau, H.; Comba, P.; Ray, K. *Angew. Chem., Int. Ed.* **2011**, *50*, 1711. (b) Yiu, S.-M.; Man, W.-L.; Lau, T.-C. *J. Am. Chem. Soc.* **2008**, *130*, 10821. (c) Lam, W. W. Y.; Yiu, S.-M.; Lee, J. M. N.; Yau, S. K. Y.; Kwong, H.-K.; Lau, T.-C.; Liu, D.; Lin, Z. *J. Am. Chem. Soc.* **2006**, *128*, 2851. (d) Yiu, S.-M.; Wu, Z.-B.; Mak, C.-K.; Lau, T.-C. *J. Am. Chem. Soc.* **2004**, *126*, 14921. (e) Miller, C. G.; Gordon-Wylie, S. W.; Horwitz, C. P.; Strazisar, S. A.; Peraino, D. K.; Clark, G. R.; Weintraub, S. T.; Collins, T. J. *J. Am. Chem. Soc.* **1998**, *120*, 11540. (f) Du, H.; Lo, P.-K.; Hu, Z.; Liang, H.; Lau, K.-C.; Wang, Y.-N.; Lam, W. W. Y.; Lau, T.-C. *Chem. Commun.* **2011**, *47*, 7143.

(6) (a) Umena, Y.; Kawakami, K.; Shen, J.-R.; Kamiya, N. *Nature* **2011**, *473*, 55. (b) Gatt, P.; Patrie, S.; Stranger, R.; Pace, R. J. *Angew. Chem., Int. Ed.* **2012**, *51*, 12025.

(7) (a) Kanady, J. S.; Tsui, E. Y.; Day, M. W.; Agapie, T. *Science* **2011**, *333*, 733. (b) Park, Y. J.; Ziller, J. W.; Borovik, A. S. *J. Am. Chem. Soc.* **2011**, *133*, 9258.

(8) Fukuzumi, S.; Morimoto, Y.; Kotani, H.; Naumov, P.; Lee, Y.-M.; Nam, W. *Nat. Chem.* **2010**, *2*, 756.

(9) (a) Morimoto, Y.; Kotani, H.; Park, J.; Lee, Y.-M.; Nam, W.; Fukuzumi, S. *J. Am. Chem. Soc.* **2011**, *133*, 403. (b) Park, J.; Morimoto, Y.; Lee, Y.-M.; Nam, W.; Fukuzumi, S. *J. Am. Chem. Soc.* **2011**, *133*, 5236.

(10) Leeladee, P.; Baglia, R. A.; Prokop, K. A.; Latifi, R.; de Visser, S. P.; Goldberg, D. P. *J. Am. Chem. Soc.* **2012**, *134*, 10397.

(11) Wu, X.; Seo, M. S.; Davis, K. M.; Lee, Y.-M.; Chen, J.; Cho, K.-B.; Pushkar, Y. N.; Nam, W. *J. Am. Chem. Soc.* **2011**, *133*, 20088.

(12) Evans, D. F.; Jakubovic, D. A. *J. Chem. Soc., Dalton Trans.* **1988**, 2927.

(13) Cho, K.-B.; Shaik, S.; Nam, W. *J. Phys. Chem. Lett.* **2012**, *3*, 2851.

(14) Direct binding of two Sc^{3+} ions to the Mn−O moiety in **4** may be unlikely to occur, since the resulting structure is 40 kcal/mol higher in energy than the one with only one bound Sc^{3+} (see Figure S15).

(15) Although **3** showed a reactivity between those of **2** and **4** in the oxidation of thioanisole, we were not able to determine an accurate rate constant because of poor kinetic fitting in the first-order decay profile for thioanisole oxidation by **3**.

(16) (a) Garcia-Bosch, I.; Company, A.; Cady, C. W.; Styring, S.; Browne, W. R.; Ribas, X.; Costas, M. *Angew. Chem., Int. Ed.* **2011**, *50*, 5648. (b) Sawant, S. C.; Wu, X.; Cho, J.; Cho, K.-B.; Kim, S. H.; Seo, M. S.; Lee, Y.-M.; Kubo, M.; Ogura, T.; Shaik, S.; Nam, W. *Angew. Chem., Int. Ed.* **2010**, *49*, 8190. (c) Jeong, Y. J.; Kang, Y.; Han, A.-R.; Lee, Y.-M.; Kotani, H.; Fukuzumi, S.; Nam, W. *Angew. Chem., Int. Ed.* **2008**, *47*, 7321.

(17) Morimoto, Y.; Park, J.; Suenobu, T.; Lee, Y.-M.; Nam, W.; Fukuzumi, S. *Inorg. Chem.* **2012**, *51*, 10025.

(18) (a) Goto, Y.; Matsui, T.; Ozaki, S.; Watanabe, Y.; Fukuzumi, S. *J. Am. Chem. Soc.* **1999**, *121*, 9497. (b) Taki, M.; Itoh, S.; Fukuzumi, S. *J. Am. Chem. Soc.* **2002**, *124*, 998. (c) Arias, J.; Newlands, C. R.; Abu-Omar, M. M. *Inorg. Chem.* **2001**, *40*, 2185. (d) McPherson, L. D.; Drees, M.; Khan, S. I.; Strassner, T.; Abu-Omar, M. M. *Inorg. Chem.* **2004**, *43*, 4036. (e) Kumar, A.; Goldberg, I.; Botoshansky, M.; Buchman, Y.; Gross, Z. *J. Am. Chem. Soc.* **2010**, *132*, 15233.